

***In Situ* FTIR Spectroscopic Analysis of Carbonate Transformations during Adsorption and Desorption of CO₂ in K-Promoted HTlc**

Hai Du, Christopher T. Williams, Armin D. Ebner, and James A. Ritter*

Department of Chemical Engineering, University of South Carolina, Columbia, South Carolina 29208

Received March 9, 2010

In situ FTIR spectroscopy was used to study carbonate transformations during adsorption and desorption of CO₂ in K-promoted HTlc at 450 °C just after activation. It revealed one irreversible process associated with the slow formation of polydentate carbonate during both adsorption and desorption, which explains CO₂ capacity fade with cycling. It also revealed several reversible processes associated with the disappearance of free carbonate ion and the formation of unidentate, bidentate, and bridged (surface) carbonates during the adsorption of gaseous CO₂ on active sites (highly basic, metal-bound unsaturated oxygen atoms) and vice versa during desorption. As the active sites became depleted during adsorption, free carbonate also transformed into bidentate, bidentate formation continued throughout adsorption, and unidentate and bridged carbonates began to disappear, possibly transforming irreversibly into polydentate. Once enough active sites became available during desorption, bidentate also began to transform back into free carbonate, unidentate and bridged carbonates continued to disappear throughout desorption, and bidentate disappearance and free carbonate formation both ceased. The slow formation of bidentate during adsorption and the slow disappearance of unidentate and bridged carbonates during desorption explains the never ending CO₂ uptake and release. Changes in active site and carbonate basicity were the driving force behind K-promoted HTlc being a reversible adsorbent for CO₂ at around 450 °C.

Introduction

Hydrotalcite-like compounds (HTlcs) belong to a large class of anionic clays that have a layered structure comprising metallic oxides (or metallic hydroxides) and carbonates.^{1,2} Because of their ability to reversibly adsorb CO₂ with reasonable working capacities simply by changing the pressure at relatively high temperatures, especially if promoted with K₂CO₃, HTlcs have been proposed for use as adsorbents for CO₂ removal in reforming³ and flue gas streams.^{4,5} However, a mechanism that explains the uptake and release of CO₂ in HTlcs has not been well established.

Recently, Ritter and co-workers^{6–8} carried out gravimetric adsorption and desorption studies of CO₂ in K-promoted HTlc and proposed a plausible mechanism that explains the behavior of this complex system. The mechanism described the dynamics of the uptake and release of CO₂ in K-promoted HTlc via a reversible

nonequilibrium kinetic model (RNEK),^{7,8} based in part on Langmuir–Hinshelwood type kinetics. This RNEK model explains very well the initially fast adsorption and desorption phenomena, followed by states of extremely slow uptake and release of CO₂ that requires hours perhaps days to reach equilibrium. However, the adsorption and desorption measurements carried out by Ritter and co-workers^{6–8} alone were not sufficient to grant validation of their proposed mechanism. Thus, additional experimental evidence is required.

Infrared (IR) spectroscopy has also been utilized to study HTlcs.^{9–13} In particular, the vibrational modes of the interlayer carbonate species within the HTlc structure have been identified.^{9–11} Moreover, thermogravimetric techniques coupled with IR have also been used to determine conditions for which reactions such as dehydration, dehydroxylation, and decarbonation take place in HTlcs.^{10–13} However, all of those studies only considered the processes taking place during the initial activation of the sample. The use of *in situ* IR to study the

*To whom correspondence should be addressed. Phone: (803) 777-3590. Fax: (803) 777-8265. E-mail: ritter@cec.sc.edu.

- (1) Cavani, F.; Trifiro, F.; Vaccari, A. *Catal. Today* **1991**, *11*, 173–301.
- (2) Hutson, N. D.; Speakman, S. A.; Payzant, E. A. *Chem. Mater.* **2004**, *16*, 4135–4143.
- (3) Hufton, J. R.; Mayorga, S.; Sircar, S. *AIChE J.* **1999**, *45*, 248–256.
- (4) Yong, Z.; Mata, V.; Rodrigues, A. E. *Sep. Purif. Technol.* **2002**, *26*, 195–205.
- (5) Ding, Y.; Alpay, E. *Trans. Inst. Chem. Eng.* **2001**, *79*, 45–51.
- (6) Ebner, A. D.; Reynolds, S. P.; Ritter, J. A. *Ind. Eng. Chem. Res.* **2006**, *45*, 6387–6392.
- (7) Ebner, A. D.; Reynolds, S. P.; Ritter, J. A. *Ind. Eng. Chem. Res.* **2007**, *46*, 1737–1744.
- (8) Du, H.; Ebner, A. D.; Ritter, J. A. *Ind. Eng. Chem. Res.* **2010**, *49*, 3328–3336.

- (9) Klopogge, J. T.; Wharton, D.; Hickey, L.; Frost, R. L. *Am. Mineral.* **2002**, *87*, 623–629.
- (10) Abelló, S.; Medina, F.; Tichit, D.; Pérez, R. J.; Groen, J. C.; Sueiras, J. E.; Salagre, P.; Cesteros, Y. *Chem.—Eur. J.* **2005**, *11*, 728–739.
- (11) Yang, W.; Kim, Y.; Liu, P. K. T.; Sahimi, M.; Tsotsis, T. T. *Chem. Eng. Sci.* **2002**, *57*, 2945–2953.
- (12) Rey, F.; Fornes, V.; Rojo, J. M. *J. Chem. Soc. Faraday Trans.* **1992**, *88*, 2233–2238.
- (13) Hibino, T.; Yamashita, Y.; Kosuge, K.; Tsunashima, A. *Clays Clay Miner.* **1995**, *43*, 427–432.

dynamics and carbonate transformation taking place during the adsorption and desorption of CO₂ in HTlcs has not been investigated.

Therefore, the objective of this study was to use *in situ* Fourier transform infrared (FTIR) spectroscopy to identify the formation and disappearance of carbonate species within K-promoted HTlc, respectively, during the adsorption and desorption of CO₂. The same experimental conditions utilized in one of the gravimetric adsorption and desorption cycling studies carried out by Ebner et al.⁷ were utilized in this work for comparison. The notion was that independent experimental measurements done under similar conditions could be used to further validate both the mechanism⁶ and RNEK model^{7,8} that describe the adsorption and desorption behavior of CO₂ in K-promoted HTlc.

Experimental Details

Synthesis of K-Promoted HTlc. An HTlc with molecular formula [Mg₃Al(OH)₈]₂CO₃·*n*H₂O was prepared by the same coprecipitation method used in the previous studies.^{6–8} While vigorously stirring, a solution of 41.7 mL of deionized water containing 0.75 mol of Mg(NO₃)₂·6H₂O and 0.25 mol of Al(NO₃)₃·9H₂O was added to a solution of 83.3 mL of deionized water containing 1.7 mol of NaOH and 0.5 mol of Na₂CO₃. The precipitate was separated from the slurry by vacuum filtration. The wet filter cake was washed with deionized water and vacuum filtered three times, dried overnight at 60 °C in a vacuum oven, crushed, and calcined in air at 400 °C for 4 h.

K-promoted HTlc with molecular formula [Mg₃Al(OH)₈]₂·CO₃·K₂CO₃·*n*H₂O was prepared using an incipient wetness procedure like before.^{6–8} To obtain an Al/K mole ratio of 1:1, a 0.33 M solution of K₂CO₃ was prepared in deionized water, and a predetermined volume was added to the HTlc powder in three steps: (1) The solution was added dropwise to the powder until it appeared wet. (2) The wet powder was dried for 15 min in a vacuum oven at 60 °C. (3) Steps 1 and 2 were repeated until all of the solution was added.

FTIR Spectroscopy Analysis. Powder samples of K-promoted HTlc were combined with oven-dried spectroscopic-grade KBr (Alfa Aesar) and pressed into self-supported wafers under 6000 psi of pressure. Each wafer contained 16.7 wt % K-promoted HTlc, had a diameter of 12 mm, and a thickness of approximately 30 mg/cm². The spectra of the samples were recorded by accumulating 64 scans at 4 cm^{−1} resolution in the spectral range of 650–4000 cm^{−1} using a Nicolet Nexus 470 FT-IR spectrometer equipped with an MCT-B detector cooled by liquid nitrogen. A 10 cm long water-cooled stainless steel IR cell, with NaCl windows, was used to collect the *in situ* spectra. A heating element inserted into the cell allowed spectra collection at elevated temperatures. The cell temperature was monitored by a K-type thermocouple placed in close proximity to the K-promoted HTlc sample.

IR spectra of a fresh sample of K₂CO₃-promoted HTlc were collected as follows. An *in situ* spectroscopic run was carried out under the same conditions as those used during the gravimetric study.⁷ First, an activation step was carried out in He (National Welders, 99.999%) flowing at 1 atm by ramping the temperature at 2 °C/min from 30 to 450 °C (i.e., 210 min) and then soaking the sample for another 120 min at 450 °C. Next, the adsorption step was carried out at 450 °C for 300 min with CO₂ (National Welders, 99.8%) flowing at 1 atm. Finally, the desorption step

was carried out at 450 °C for 300 min with He flowing at 1 atm. For every collection, the spectrum of the gas phase was collected first as the background prior to each measurement to eliminate its affect. Prior to each experiment, the sample was pretreated at room temperature for 1 h in He flowing at 1 atm. The gas flow rate through the IR cell was always maintained at 60 mL (STP)/min.

Results and Discussion

Three processes were carried out experimentally in this study, as described above. First, the sample was activated for 330 min by heating it from 30 to 450 °C in He. This removed most of the bound H₂O and hydroxyl groups as H₂O and some of the bound carbonate species as CO₂. Second, the sample was subjected to CO₂ at 450 °C for 300 min to observe the uptake of CO₂ through changes that occurred in the type and amount of carbonate species within the structure. Third, the sample was subjected to He at 450 °C for 300 min to observe the release of CO₂ again through changes that occurred in the type and amount of carbonate species within the structure.

The chemical transformations that took place during the activation process were essentially the same as those described in the literature;^{10–13} thus, they are discussed here only briefly to help facilitate the discussion later on a proposed mechanism. It is well documented that as the temperature increases chemisorbed water is released first, followed by dehydroxylation, and then by both dehydroxylation and decarbonization. In the 300 to 450 °C range, the species remaining in the interlayers include metal-bound hydroxyl groups, free carbonate ions, and metal-coordinated unidentate, bidentate, and bridged carbonates species.^{2,11,12} Polydentate carbonate is also present but in the bulk of the structure.^{14,15} Some restructuring of the solid also occurs, giving rise to metal-bound unsaturated oxygen atoms among the Mg, Al, and in this case K atoms.^{16,20}

Table 1 lists the approximate wave numbers and splitting differences of the ν₃ vibration (Δν₃) reported in the literature^{15,17–22} for the five aforementioned carbonate species on various metal oxides, including HTlcs. Figure 1a and b shows the FTIR spectra of K-promoted HTlc collected in the range identified in Table 1 (1900 and 1200 cm^{−1}) at eight different times during the 300 min adsorption step and at eight different times during the 300 min desorption step, respectively. Figure 2 contrasts the FTIR spectra of K-promoted HTlc at the beginning of the 300 min adsorption step with that at end of the 300 min

- (14) Daturi, M.; Binet, C.; Lavalley, J. C.; Galtayries, A.; Sporken, R. *Phys. Chem. Chem. Phys.* **1999**, *1*, 5717–5724.
- (15) Lavalley, J. C. *Catal. Today* **1996**, *27*, 377–401.
- (16) Xie, W.; Peng, H.; Chen, L. *J. Mol. Catal. A: Chem.* **2006**, *246*, 24–32.
- (17) Evans, J. V.; Whateley, T. L. *Trans. Faraday Soc.* **1967**, *63*, 2769–2777.
- (18) Busca, G.; Lorenzelli, V. *Mater. Chem.* **1982**, *7*, 89–126.
- (19) Prescott, H. A.; Li, Z. J.; Kemnitz, E.; Trunschke, A.; Deutsch, J.; Lieske, H.; Auroux, A. *J. Catal.* **2005**, *234*, 119–130.
- (20) Cosimo, J. I. Di; Diez, V. K.; Xu, M.; Iglesia, E.; Apesteguia, C. R. *J. Catal.* **1998**, *178*, 499–510.
- (21) Philipp, R.; Fujimoto, K. *J. Phys. Chem.* **1992**, *96*, 9035–9038.
- (22) Lercher, J. A.; Colombier, C.; Noller, H. *J. Chem. Soc. Faraday Trans.* **1984**, *80*, 949–959.

Table 1. IR Band Positions (cm^{-1}) of Different Carbonate Species on Various Metal Oxides

Reference	Metal Oxide	Vibration Mode	Carbonate Ion	Unidentate	Bidentate	Bridged	Polydentate
17	MgO	ν_1	1020-1090	1040-1080	1020-1030		
		ν_2	860-880				
		ν_3	ν_{as}	1470-1530	1590-1630		
			ν_s	1300-1370	1260-1270		
		ν_4	680-750				
18	MgO	ν_1	1063	1050	1005-950		
		ν_2	879	860	850-830		
		ν_3	ν_{as}	1520-1550	1625-1670		
			ν_s	1390-1410	1275-1325		
		ν_4	680				
	Al ₂ O ₃	ν_3	ν_{as}	1610-1570	1710-1660	1730-1810	
			ν_s	1385-1350	1310-1345	1310	
19	Al ₂ O ₃	ν_3	ν_{as}	1450	1704	1756	
			ν_s		1265	1204	
	MgO	ν_3	ν_{as}	1525-1578	1630	1686	1444
			ν_s	1381	1304	1217	1365
	CHT ^a	ν_3	ν_{as}	1574-1591	1650-1658		
20	CHT ^a	ν_3	ν_s	1365-1386	1400-1420		
			ν_{as}	1510-1560	1610-1630		
21	MgO /CaO	ν_3	ν_{as}	1506-1560		1776-1781	
			ν_s	1360-1419			
22	Al ₂ O ₃ /MgO	ν_3	ν_{as}	1538-1580	1700		
			ν_s	1420	1357-1380		
15,18		$\Delta\nu_3 (\nu_{as}-\nu_s)$		~100	~300	>400	<100

^aCHT: calcined hydrotalcite (> 400 °C, in N₂ or air).

desorption step. Changes in the IR spectra were clearly taking place during both adsorption and desorption (Figure 1), with slight differences remaining even after a complete adsorption and desorption cycle (Figure 2). On the basis of the information in Table 1, a wavenumber band was assigned to each carbonate species to identify the relative change in each carbonate species during adsorption and desorption. These wavenumber bands are indicated in Figure 1.

For the IR spectra in Figure 1, band component analysis was done at each time using a Gaussian function^{23,24} given by

$$f_G(\nu) = I_0 \exp\left(-\frac{4\ln 2}{\sigma^2}(\nu - \nu_0)^2\right) \quad (1)$$

where I_0 is the band height, ν_0 is the wavenumber, and σ is the bandwidth at $I_0/2$ for each band. Equation 1 was fitted

to the experimental IR spectra in two stages. The first stage was used to obtain initial guesses for each of the parameters by fitting eq 1 only to the IR spectrum taken at 300 min into the adsorption process. It was surmised that most, if not all, of the carbonate species would be present in the sample at 300 min, i.e., at the end of adsorption. This was done by varying I_0 , σ and ν_0 for each band while minimizing the sum of the square error between the experimental and predicted IR spectra. During the regression process, ν_0 was restricted to the range of the literature values listed in Table 1, σ was restricted to $20 < \sigma < 300$, and $I_{0,as}/I_{0,s}$ was restricted to $0.3 < I_{0,as}/I_{0,s} < 3$.

The second stage used the resulting parameters from stage one as initial guesses for finding the set of parameters that minimized the sum of the square error between the experimental and predicted IR spectra simultaneously for all 15 IR scans collected at the various times during adsorption and desorption. This was done by allowing I_0 for each band to vary in time as needed, by allowing σ and ν_0 to vary only slightly about their stage one values but remain constant in time for each band, and by keeping $I_{0,as}/I_{0,s}$ constant for each band at their stage one value.

(23) Buslov, D. K.; Nikonenko, N. A.; Sushko, N. I.; Zhabankov, R. G. *J. Appl. Spectrosc.* **2001**, 68, 917–923.

(24) Domke, W. D.; Steinke, H. J. *Polym. Sci., Part A: Polym. Chem.* **1986**, 24, 2701–2705.

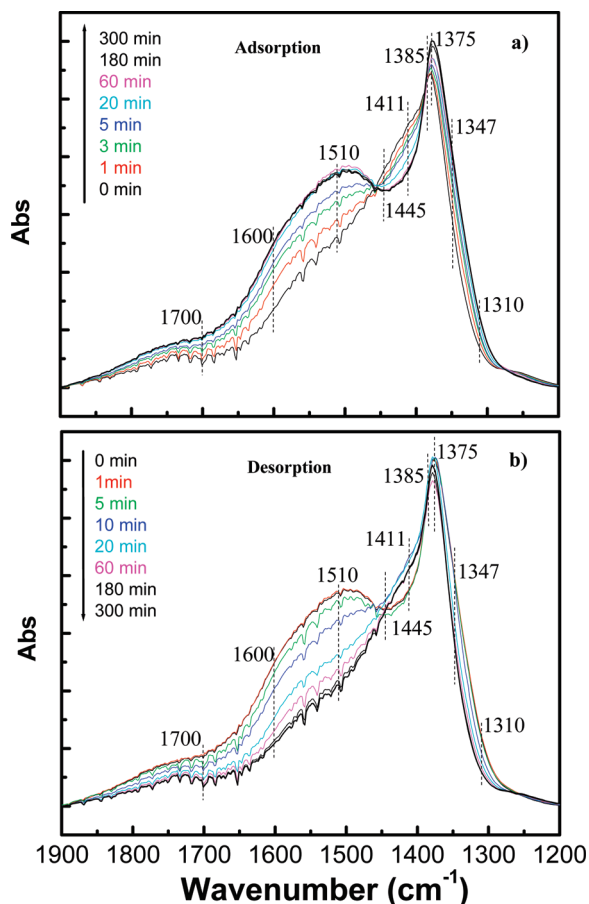


Figure 1. FTIR spectra for K-promoted HTlc collected at different times while being exposed to (a) 1 atm of CO₂ for 300 min at 450 °C just after activation to facilitate CO₂ adsorption (upper figure) and while being exposed to (b) 1 atm of He for 300 min at 450 °C just after adsorption to facilitate CO₂ desorption (lower figure). The IR spectra for 300 min into CO₂ adsorption is the same as the IR spectra for 0 min into CO₂ desorption.

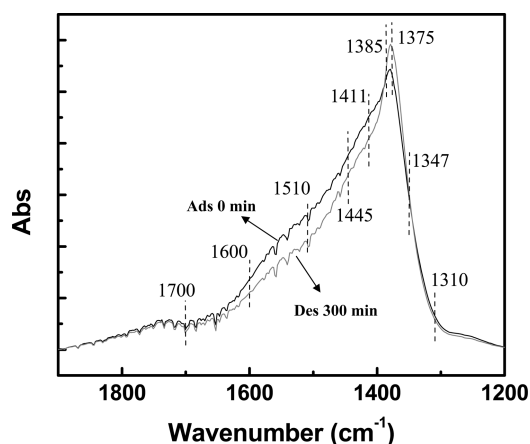


Figure 2. FTIR spectra for K-promoted HTlc collected just prior to having the sample exposed to 1 atm of CO₂ for 300 min at 450 °C (0 min curve in Figure 1a) and just after having the sample exposed to 1 atm of He for 300 min at 450 °C (300 min curve in Figure 1b).

The resulting fits of eq 1 to the experimental IR spectra during adsorption and desorption are shown in Figure 3 for some of the times, along with the component bands for each species. The correlation of eq 1 with the experimental data was considered to be excellent, especially

when considering the number of parameters that had to be regressed and that the regression was done simultaneously with all 15 scans. The corresponding band positions, band widths, and band height ratio of the component bands in Figure 3 are listed in Table 2 for each carbonate species. These parameter ranges agreed very well with the ranges from the literature shown in Table 1, which lent credence to the band component analysis and the supposition that the five carbonate species listed in Table 1 were actually present in the K-promoted HTlc sample.

To show the relative change of each carbonate species during adsorption and desorption, the area under each band in Figure 3 was calculated and plotted in Figure 4. The resulting curves were arbitrarily shifted in the area axis for better viewing. Note that since the sensitivity of the IR area varies for each carbonate species the magnitude of these results could be used only to observe the change in a species relative to itself over time but not relative to another species. The trends in Figure 4 clearly showed that one irreversible and several reversible processes were taking place during both adsorption and desorption. The irreversible process was associated with the polydentate carbonate steadily increasing in time with relatively slow kinetics throughout the adsorption and desorption steps. This irreversibility is perhaps related to the slight loss of CO₂ capacity observed in HTlcs with CO₂ adsorption and desorption cycling.^{7,8}

In contrast, the reversible processes all involved the other carbonate species, and displayed trends that were consistent with the three-step kinetic mechanism proposed by Ebner et al.^{6–8} based on gravimetric experiments. For example, from 1 to 5 min during CO₂ adsorption, the free carbonate ion decreased drastically, while the unidentate, bidentate, and bridged (surface) carbonates all increased significantly. From 5 to 60 min during CO₂ adsorption, both the disappearance of the free carbonate ion and the formation of the three surface carbonates slowed down. From 60 to 300 min during CO₂ adsorption, the rates of change of all four carbonates slowed significantly and were characterized by a linear trend, with reversal observed by the unidentate and bridged carbonates. Similar rate processes were observed during CO₂ desorption but with the trends reversed and the first two of the three kinetic processes each a little bit slower compared to adsorption.

The opposite trend observed between the area of the free carbonate ions and those of the other three carbonates (i.e., unidentate, bidentate and bridged) revealed the formation and disappearance of stable free carbonate ion when in the absence and presence of gaseous CO₂, respectively. Since more free carbonate ions were present in the absence of gaseous CO₂, it was envisioned that the free carbonate ion at the end of activation interacted quite favorably with the abundance of a variety of highly basic, metal-bound unsaturated oxygen atoms that formed as a consequence of CO₂ desorption. When CO₂ adsorption took place, these metal-bound

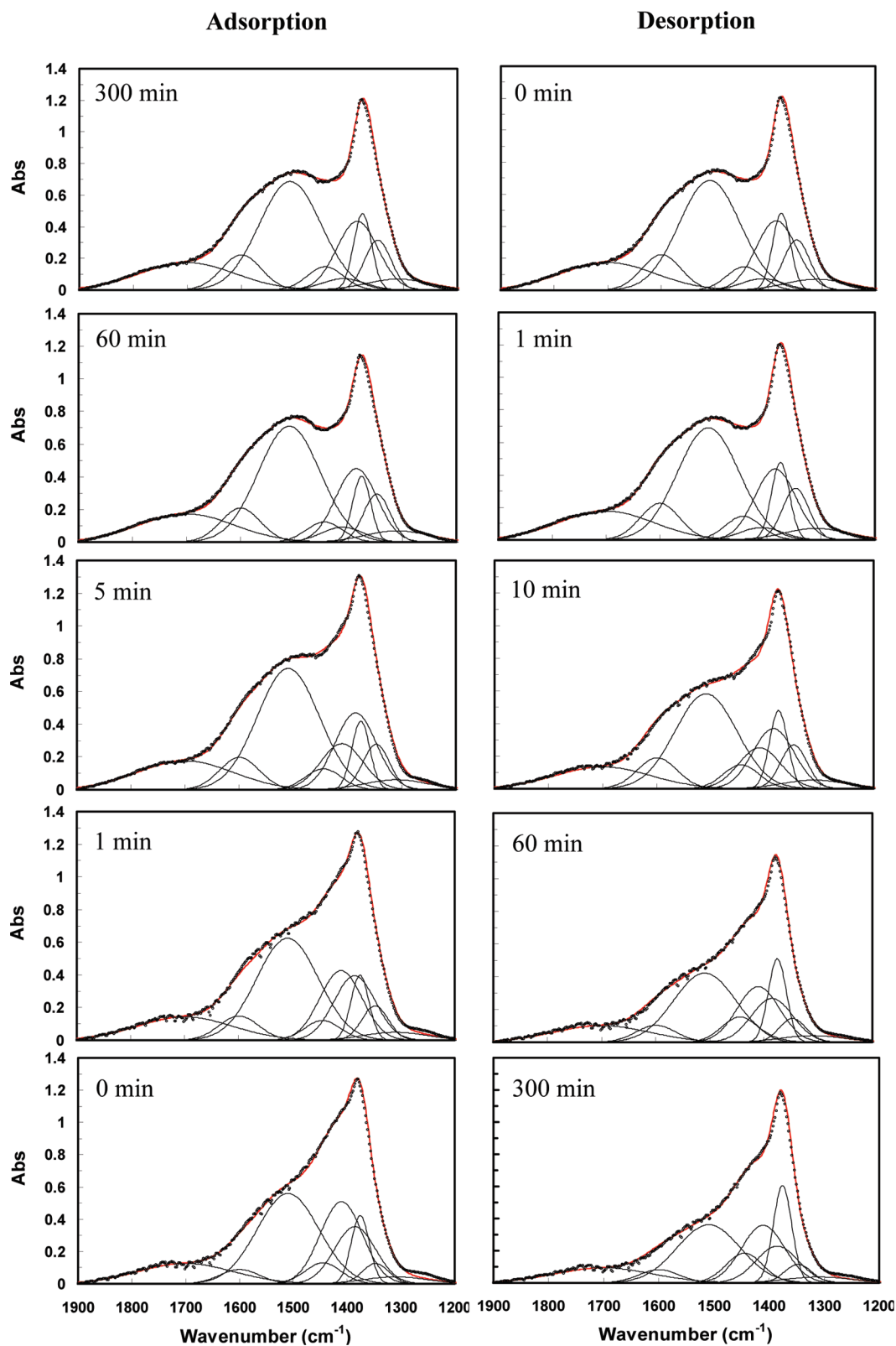


Figure 3. Band component analysis of each FTIR spectrum collected for K-promoted HTlc at different times while being exposed to 1 atm of CO₂ for 300 min at 450 °C just after activation to facilitate CO₂ adsorption (left column of figures) and while being exposed to 1 atm of He for 300 min at 450 °C just after adsorption to facilitate CO₂ desorption (right column of figures). Symbols, experimental FTIR spectra; solid lines, fitted FTIR spectra and resulting peaks from band component analysis. The figure for 300 min into CO₂ adsorption is the same as the figure for 0 min into CO₂ desorption.

unsaturated oxygen atoms became saturated by forming unidentate, bidentate, and bridged carbonates. This reduced the chances for the free carbonate ion to interact freely with the metal-bound unsaturated oxygen sites,

perhaps transforming it into one or more of the surface carbonates.^{11,16,20}

To expound on a possible mechanism that perhaps explains these carbonate transformations, the results in

Table 2. IR Band Positions Determined for Each Carbonate Species from the Band Component Analysis of All the FTIR Spectra for K-Promoted HTlc Collected at 15 Different Times during CO₂ Adsorption and Desorption

carbonate species	free ion	bulk polydentate		surface unidentate		surface bidentate		surface bridged	
		$\nu_{as}(\text{CO}_3)$	$\nu_s(\text{CO}_3)$	$\nu_{as}(\text{CO}_3)$	$\nu_s(\text{CO}_3)$	$\nu_{as}(\text{CO}_3)$	$\nu_s(\text{CO}_3)$	$\nu_{as}(\text{CO}_3)$	$\nu_s(\text{CO}_3)$
band position (cm ⁻¹)	1411	1445	1375	1510	1385	1600	1347	1700	1310
band width (cm ⁻¹)	92.2	78.4	39.2	134.9	89.9	86.2	57.4	206.6	137.7
band height ratio for pair species (ν_{as}/ν_s)		0.3		1.6		0.71		2.6	

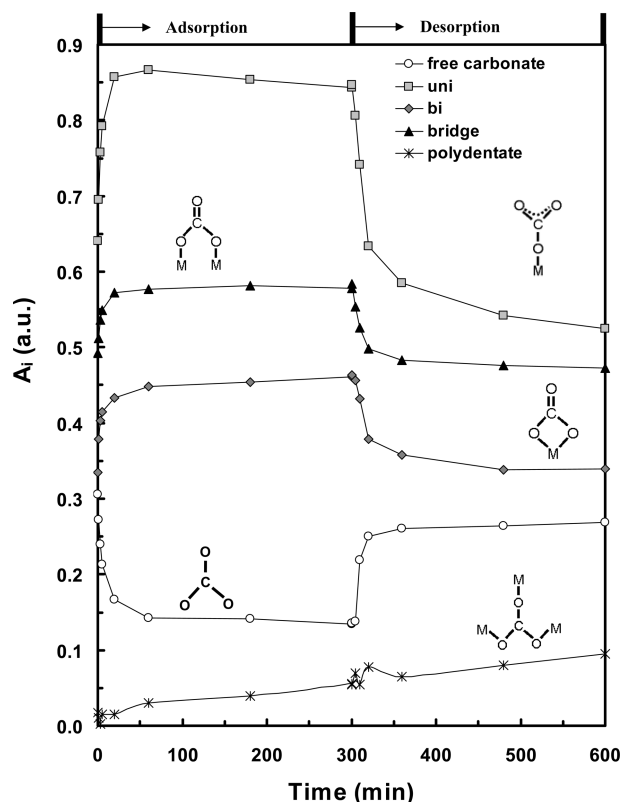
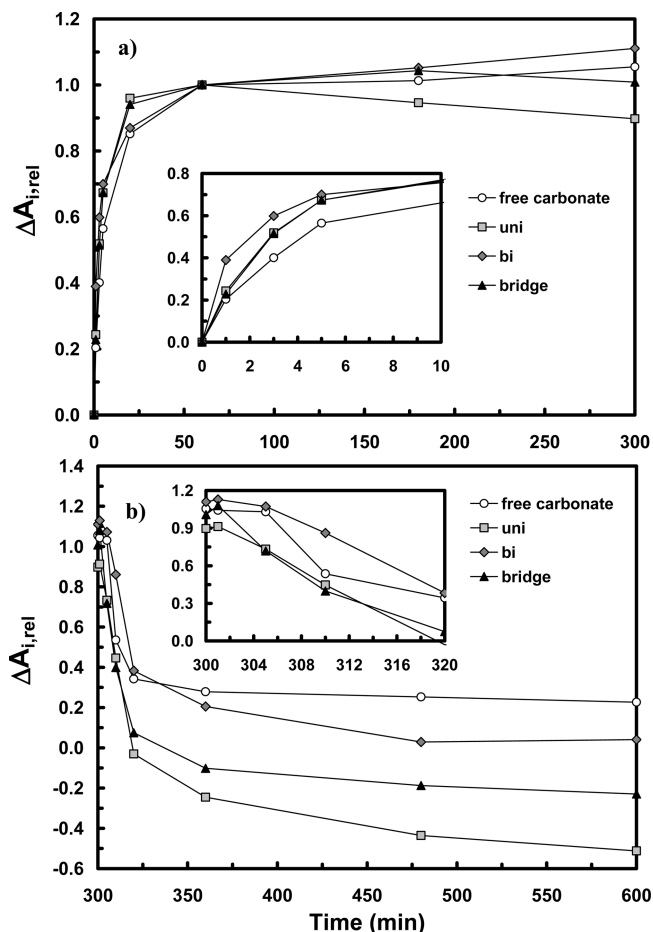
**Figure 4.** Integrated areas from the band component analysis of each FTIR spectrum collected for K-promoted HTlc at different times while being exposed to 1 atm of CO₂ for 300 min at 450 °C just after activation to facilitate CO₂ adsorption and while being exposed to 1 atm of He for 300 min at 450 °C just after adsorption to facilitate CO₂ desorption.

Figure 4 were scaled to make all the relative areas equal at 60 min according to the following formula:

$$\Delta A_{i,rel} = \frac{A_i(t) - A_i(t = 0\text{min})}{A_i(t = 60\text{min}) - A_i(t = 0\text{min})} \quad (2)$$

where $A_i(t)$, $A_i(t = 0\text{ min})$ and $A_i(t = 60\text{ min})$ correspond to the areas displayed by species i at any time t , $t = 0\text{ min}$ and $t = 60\text{ min}$ in Figure 4, respectively. The resulting plots are displayed in Figure 5 for both the adsorption and desorption steps. The inserts provide an expanded view of the results within the first few minutes of each step. The results in Figure 5 were used to readily compare the relative changes in areas exhibited by each of these species, which corresponds directly to the rates of formation and disappearance of each carbonate.

During the first minute of the adsorption step, the rate of formation of the bidentate carbonate was nearly twice that of the formation of unidentate or bridged carbonate, both of which exhibited nearly identical rates. However, after 1 min the rate of formation of the bidentate carbonate

**Figure 5.** Integrated areas shown in Figure 4 scaled according to eq 2. Inserts show expanded views of the areas at short times during adsorption and desorption.

decreased significantly and was slower than that of unidentate or bridged carbonate. This result was significant because it revealed the existence of at least two different active sites: those that favored the formation of bidentate carbonate and those that favored the formation of unidentate and bridged carbonates. In contrast, during the early minutes of the desorption step, the rate of disappearance of bidentate carbonate lagged behind the almost identical rates of disappearance of both unidentate and bridged carbonates. In fact, bidentate carbonate started disappearing only after 4 min into the desorption step, while unidentate and bridged carbonates started disappearing immediately. It seemed evident that the early preference toward bidentate carbonate formation during adsorption and then its slower disappearance during desorption were associated with unique sites that led to a more favorable thermodynamic state compared to other sites; this supposition is contrary to that reported elsewhere.²⁰

Moreover, it was quite intriguing that throughout both the adsorption and desorption steps, the rates of change of free carbonate ion were very similar to those of bidentate carbonate, perhaps suggesting that the free carbonate ion originated mostly from bidentate carbonate.

After 60 min into the adsorption step, the kinetics of all of the carbonates, with the exception of bridged carbonate, clearly followed a linear change in time. However, the unidentate carbonate trend was reversed, with its area decreasing in time. For bridged carbonate, this reversal also occurred but only after 200 min. In contrast, after 60 min into the desorption step, the linear trends were not as clearly defined for any of the carbonates. Nevertheless, it was clear that after around 20 and 35 min into desorption, the intensities for both unidentate and bridged carbonates, respectively, became smaller than those at the beginning of the adsorption step (i.e., at $t = 0$ min). These results were consistent with the differences observed between the IR spectra shown in Figure 2. It was speculated that the latter was associated with the reversal exhibited by these carbonates at the later stages of the adsorption step. Again, it was quite intriguing that, similar to the early stages of adsorption and desorption, both bidentate carbonate and the free carbonate ion followed similar kinetic trends during the much later stages.

On the basis of the above observations, a plausible mechanism was devised for these carbonate transformations. Just after activation, the surface of K-promoted HTlc is characterized principally by active sites, likely comprising different forms of highly basic, metal-bound unsaturated oxygen atoms formed during the activation process^{16,20,25} and free carbonate ion stabilized by this excess of active sites. There are also unidentate, bidentate, and bridged carbonates present in appreciable quantities. At the start of the adsorption process, gaseous CO₂ molecules rapidly chemisorb to certain active sites forming more unidentate, bidentate, and bridged carbonates, while favoring bidentate formation at short times and probably on the more active sites. This, in turn, fosters a reduction in the number of free carbonate ions because the number of stabilizing active sites becomes depleted. The faster formation of bidentate carbonate initially compared to that of unidentate and bridged carbonates, without the latter serving as intermediates, may be explained by some of the active sites having a conformational characteristic that facilitates favorable kinetics and thermodynamics for bidentate formation. This explanation is consistent with the fact that bidentate carbonate is less basic (or more neutral) than unidentate and bridged carbonates,^{20,25,26} making its formation more stable and thus more favorable. In contrast, unidentate and bridged carbonates, through gaseous CO₂ chemisorption, seem to form at almost identical rates most likely on the less energetic sites. It is envisioned that the highly energetic

sites leading to bidentate carbonate formation are much less abundant and thus become depleted faster than the less energetic ones. This explains why the rate of formation of bidentate carbonate is significantly reduced after the first minute, while the rates of formation of both unidentate and bridged carbonates remain relatively faster for another 20 min.

The similar shapes of the curves for the free carbonate ion and bidentate carbonate also suggest that after the first minute of adsorption, the bidentate carbonate is no longer just formed through gaseous CO₂ chemisorption but that it is also formed by the free carbonate ion transforming into bidentate carbonate, as the highly energetic sites it favorably interacts with become depleted. This conversion of free carbonate ion into bidentate carbonate seems to continue for the entire 300 min of adsorption. In contrast, during desorption its conversion is completely reversed, i.e., the bidentate carbonate transforms back into the free carbonate ion during the entire desorption step, as the kinetic curves for both species remain very similar also during that period.

After 60 and 180 min into the adsorption step, the number of unidentate and bridged carbonates, respectively, reach a maximum and start to decrease. This is perhaps due to a conversion of these species into bidentate carbonate, or perhaps it is due to the irreversible formation of bulk polydentate carbonate, which occurs throughout the adsorption and desorption steps. Recall that these are the only two species whose signal during the desorption step becomes less than that at the beginning of the adsorption step, favoring the notion of the conversion to polydentate.

Desorption is also characterized by an immediate conversion of unidentate and bridged carbonates into gaseous CO₂. In contrast, bidentate carbonate transformation takes place only after about 4 min into the desorption step, which is about the same time the free carbonate ion starts to form again. This delay is probably associated with the formation of a sufficient number of active sites, through unidentate and bridged carbonates transforming into gaseous CO₂, that facilitates the transformation of bidentate carbonate back into the free carbonate ion, most likely on the more highly energetic sites. As desorption continues, it is plausible that the mobility of the free carbonate ion around these highly energetic sites leaves some of them exposed and thus available for subsequent CO₂ chemisorption during the next adsorption step.

Conclusions

A study was carried out using *in situ* Fourier transform infrared (FTIR) spectroscopy to further ascertain the behavior of CO₂ during its uptake in and release from K-promoted HTlc at 450 °C. First, the sample was activated in He, then it was exposed to CO₂ to facilitate CO₂ adsorption, and finally, it was exposed to He to facilitate CO₂ desorption. The goal was to observe the formation and disappearance of different carbonate species over time during consecutive adsorption and desorption steps just after activation.

(25) Morterra, C.; Ghiotti, G.; Boccuzzi, F.; Coluccia, S. J. *Catal.* **1978**, *51*, 299–313.

(26) Collins, S. E.; Baltanás, M. A.; Bonivardi, A. L. J. *Phys. Chem. B* **2006**, *110*, 5498–5507.

The species present after activation were various forms of metal-bound unsaturated oxygen atoms, free carbonate ions, unidentate, bidentate, and bridged surface carbonates, and bulk polydentate carbonate. During subsequent CO₂ adsorption and desorption, the IR spectra revealed that one irreversible process and several reversible processes were taking place. The irreversible process was associated with bulk polydentate carbonate continuously forming very slowly during both adsorption and desorption. This might explain the slight irreversibility (fade) in the CO₂ capacity observed in previous studies during gravimetric cycling studies.

For the reversible processes taking place during a 300 min adsorption step, the following was surmised. Gaseous CO₂ molecules chemisorbed to various active sites (highly basic metal-bound unsaturated oxygen atoms formed during activation) forming unidentate, bidentate, and bridged carbonates, while favoring bidentate carbonate formation at very short times. As the active sites became depleted, free carbonate ion also transformed into bidentate carbonate. Bidentate carbonate formation continued throughout the adsorption step, while unidentate and bridged carbonates began to disappear after about 60 min, possibly transforming irreversibly into bulk polydentate carbonate.

For the reversible processes taking place during a subsequent 300 min desorption step, the following was surmised. Unidentate and bridged carbonates transformed immediately into gaseous CO₂, with bidentate carbonate transformation into gaseous CO₂ lagging behind

by a few minutes. Once enough active sites became available, bidentate carbonate also began to transform back into free carbonate ion. Unidentate and bridged carbonates continued to disappear throughout the desorption step, while bidentate carbonate disappearance and free carbonate ion formation both ceased.

The rate processes taking place during both adsorption and desorption were similar to the three step mechanism proposed in previous studies. The slow but continuous formation of bidentate carbonate during adsorption and the slow but continuous disappearance of both unidentate and bridged carbonates during desorption were especially intriguing. These exceedingly slow processes might explain the never ending CO₂ uptake and release trends observed gravimetrically also in previous studies.

Overall, it appeared that highly basic sites (i.e., the active sites) reversibly transformed into sites of less basicity (i.e., the surface carbonates) during adsorption. These changes in basicity were thought to be the thermodynamic driving force behind the carbonate transformations. They were also thought to be a key factor in making K-promoted HTlc a reversible adsorbent for CO₂ at temperatures of around 450 °C.

Acknowledgment. We gratefully acknowledge the financial support provided by the DOE through Grant No. DE-FG26-03NT41799 and the Center for Clean Coal at the University of South Carolina.